Electrophysiological Characterization of the Mechanosensitive Channel MscCG in *Corynebacterium glutamicum*

Yoshitaka Nakayama,[†*] Kenjiro Yoshimura,[‡] and Hidetoshi Iida[†*]
[†]Department of Biology, Tokyo Gakugei University, Tokyo, Japan; and [‡]Department of Biology, University of Maryland, College Park, Maryland

ABSTRACT *Corynebacterium glutamicum* MscCG, also referred to as NCgl1221, exports glutamate when biotin is limited in the culture medium. MscCG is a homolog of *Escherichia coli* MscS, which serves as an osmotic safety valve in *E. coli* cells. Patch-clamp experiments using heterogeneously expressed MscCG have shown that MscCG is a mechanosensitive channel gated by membrane stretch. Although the association of glutamate secretion with the mechanosensitive gating has been suggested, the electrophysiological characteristics of MscCG have not been well established. In this study, we analyzed the mechanosensitive gating properties of MscCG by expressing it in *E. coli* spheroplasts. MscCG is permeable to glutamate, but is also permeable to chloride and potassium. The tension at the midpoint of activation is 6.68 ± 0.63 mN/m, which is close to that of MscS. The opening rates at saturating tensions and closing rates at zero tension were at least one order of magnitude slower than those observed for MscS. This slow kinetics produced strong opening-closing hysteresis in response to triangular pressure ramps. Whereas MscS is inactivated under sustained stimulus, MscCG does not undergo inactivation. These results suggest that the mechanosensitive gating properties of MscCG are not suitable for the response to abrupt and harmful changes, such as osmotic downshock, but are tuned to execute slower processes, such as glutamate export.

INTRODUCTION

Escherichia coli cells possess three types of mechanosensitive channels—MscL, MscS, and MscM—based on the conductance. The channel activities are due to MscL and six MscS-type proteins: MscS, MscK, YbdG, YnaI, YbiO, and YjeP (1–3). These mechanosensitive channels have different thresholds of membrane tension and channel conductances, and release small intracellular molecules to reduce osmotic pressure when the cells are challenged with an osmotic downshock. Thus, they have been regarded as osmotic safety valves (4). The gating at different membrane tensions enables these channels to regulate osmolarity over a wide range of osmotic stresses. Electrophysiological experiments have shown that MscS opens at a moderate tension (5–8 mN/m) (5,6), which is above the threshold of MscM (7) but below that of MscL (10–14 mN/m) (8). The fast activation kinetics of MscS is probably advantageous for responding to an abrupt tension change caused by mechanical stress, such as hypoosmotic shock. On the other hand, adaptive behaviors of MscS, such as desensitization and inactivation, may prevent excessive efflux of intracellular molecules (9).

MscS homologs are found in various prokaryotes and eukaryotes, and are classified into 15 subfamilies based on the domain structures (10). *E. coli* MscS is a homoheptamer composed of a subunit of 286 amino acid residues with three transmembrane (TM) segments and a large carboxyl-terminal domain (see Fig. 1, *A* and *B*). The carboxyl-terminal domain constitutes a cage at the intracellular side. The third TM segment (TM3) and the adjacent carboxyl-terminal domain (cage roof) display the best homology between MscS family proteins as a conserved domain (11) (see Fig. 1, *A* and *C*). MscCG (NCgl1221) of the Gram-positive bacteria *Corynebacterium glutamicum* (533 aa) is larger than its *E. coli* MscS homolog (286 aa) due to a 247-residue C-terminal extension. Whereas MscS is primarily responsible for the response to hypoosmotic stress, MscCG has been characterized as a mechanosensitive channel for the adaptation to hyperosmotic stress. The osmolarity generated by a compatible solute, betaine, is tuned by MscCG and the betaine transporter BetP (12). A previous electrophysiological study reported that MscCG has lower conductance than MscS and slightly favors cations over anions (P_K/P_{Cl}~3.0), whereas MscS shows anion selectivity (P_{Cl}/P_K~1.5–3.0) (6,12).

Besides being an osmoregulator, MscCG is also known as a glutamate exporter. *C. glutamicum* cells secrete a large amount of glutamate through MscCG when incubated under biotin-limited conditions (13,14). Monosodium glutamate (MSG) elicits a taste known as umami and is widely used as a flavor enhancer (15). Industrially, MSG is produced by fermentation by *C. glutamicum* (16,17). Biotin limitation inhibits fatty acid synthesis and decreases the availability of phospholipids (18). Glutamate secretion can also be induced by the addition of fatty acid ester surfactants, such as Tween 40 (19). Because these treatments affect the cell-surface structure, changes in membrane tension are believed to be a key factor in glutamate secretion (20). Patch-clamp experiments using a *Bacillus subtilis* giant provacuole expressing MscCG have shown that MscCG is activated by membrane stretch (21) and releases glutamate from the cytoplasm by passive diffusion (22). Disruption of the MscCG gene resulted in the accumulation of glutamate (13), but a gain-of-function mutation that decreased the tension threshold

Submitted March 4, 2013, and accepted for publication June 27, 2013.
*Correspondence: y_nakayama9339@nifty.com or iida@u-gakugei.ac.jp
Editor: Chris Lingle.

0006-3495/13/09/1366/10 $2.00
http://dx.doi.org/10.1016/j.bpj.2013.06.054

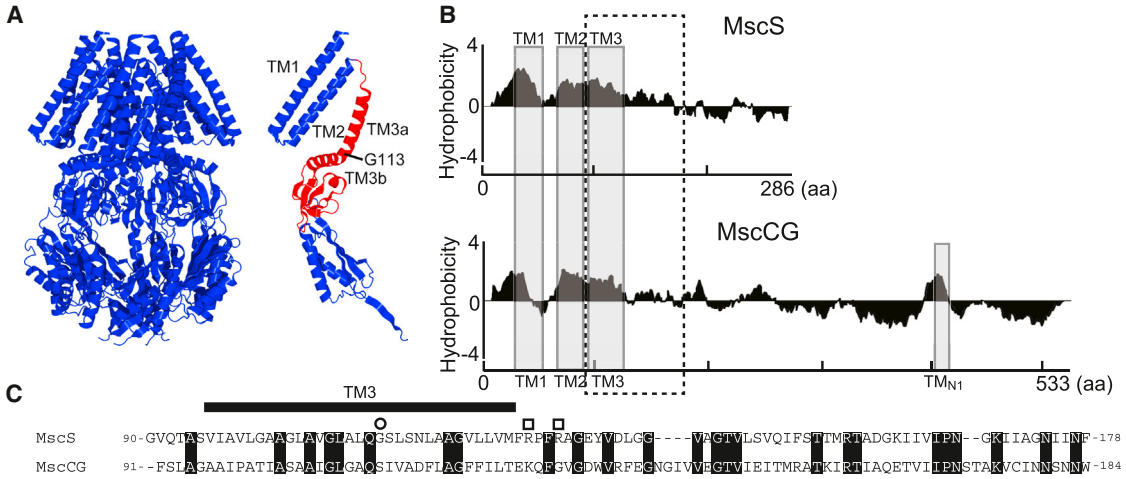

FIGURE 1 Structural features of MscS and MscCG. (*A*) Crystal structure (36) of the whole channel (*left*) and a single subunit (*right*) of the *E. coli* MscS. The red region shows the domain conserved among MscS family proteins. Gly-113 forms a kink in the inactivated state and separates TM3 into TM3a and TM3b. (*B*) Hydropathy plot of MscS and MscCG. Gray boxes show predicted TM segments. The dashed box shows the domain conserved among MscS family proteins. (*C*) The amino acid sequence alignment between MscS and MscCG in the domain conserved among MscS family proteins. Identical residues are highlighted. A glycine residue at the kink and arginine residues that form a salt bridge with the cytoplasmic cage are shown as a circle and squares, respectively.

caused constitutive glutamate secretion even in the presence of biotin (23). These results suggest that glutamate secretion in *C. glutamicum* is closely associated with the mechanosensitive gating of MscCG. However, the mechanosensitive properties of MscCG have not been fully characterized.

In this study, we analyzed the gating kinetics and ion permeability of MscCG in *E. coli* giant spheroplasts. We found that MscCG has a threshold tension close to that of MscS and shows remarkably slow gating kinetics in response to changes in membrane tension. MscCG displayed more evident hysteretic gating behavior than MscS because of this slow kinetics. Unexpectedly MscCG stayed open under sustained tension, suggesting a lack of desensitization and inactivation, as also shown previously (12). These observations suggest functional differences between *C. glutamicum* MscCG and *E. coli* MscS.

MATERIALS AND METHODS

Bacterial strains

The *E. coli* strains PB113 (Δ*mscS* and Δ*mscK*) (1) and MJF612 (Δ*mscM*, Δ*mscS*, Δ*mscK*, and Δ*mscL*) (7) were used for electrophysiological experiments, and the *E. coli* strain XL10gold (Stratagene) was used for cloning.

Giant spheroplast preparation

Patch-clamp experiments were performed on *E. coli* giant spheroplasts as described previously (24). The *MscCG* gene (also referred to as *NCgl1221*) was cloned from the *C. glutamicum* strain ATCC13869. PB113 and MJF612 cells harboring an expression vector (pB10b-MscCG or MscS) were grown for 2.5 h in the presence of cephalexin, and MscCG expression was subsequently induced for 30 min by the addition of 1 mM isopropyl-β-D-thiogalactoside (IPTG). The cells were harvested and digested with lysozyme. Spheroplasts were collected by centrifugation.

Electrophysiological recording and data analysis

We recorded the channel activity by using the inside-out, excised patch-clamp method with *E. coli* giant spheroplasts. The pipette solution contained 200 mM K-glutamate and a base salt mix (90 mM $MgCl_2$, 10 mM $CaCl_2$, and 5 mM HEPES-KOH, pH 7.2), and the bath solution contained 200 mM K-glutamate, the base salt mix, and 0.3 M sucrose to stabilize the spheroplasts. The bulk conductivities of the solutions were measured with a pH/conductivity meter (F-74; HORIBA, Japan). Currents were amplified with an Axopatch 200B amplifier (Axon Instruments, Foster City, CA) and filtered at 2 kHz. Current recordings were digitized at 5 kHz using a Digidata 1322A interface with pCLAMP9 software (Axon). Pressure applied to the patch membrane was controlled by means of a High-Speed Pressure Clamp-1 apparatus (HSPC-1; ALA Scientific Instruments, Westbury, NY) (25).

The probability of channels being open was plotted against the negative pressure (suction) applied to the patch membrane and fitted to a Boltzmann distribution function of the form $I = I_{max}/[1 + \exp \alpha (P_{mid} - P)]$, where I is the current, I_{max} is the maximum current, P is the negative pressure applied to the patch membrane, P_{mid} is the activation midpoint, and α is the channel sensitivity to pressure. The energetic and spatial parameters of MscCG and MscS were determined by the formula of a two-state Boltzmann function, $P_o = 1/[1 + \exp(\Delta E - \gamma \Delta A)/kT]$, where P_o is the probability of being open, ΔE is the free energy for a closed-to-open state transition in the absence of tension, γ is membrane tension, ΔA is the in-plane expansion, k is the Boltzmann constant, and *T* is the absolute temperature (8). The partial area changes from the closed (C) or open (O) state to the nearest transition barrier (B) were estimated from the tension dependencies of the opening and closing rates, $\Delta A_{C \to BC} = kT \times \Delta \ln(k_{on})/\Delta\gamma$ and $\Delta A_{O \to BO} = kT \times \Delta \ln(k_{off})/\Delta\gamma$, respectively, where k_{on} is the rate constant for channel opening and k_{off} is the rate constant for channel closing (9,26). BC and BO indicate the rate-limiting energy barrier closest to the closed and open states, respectively, and thus $\Delta A_{C \to BC}$ and $\Delta A_{O \to BO}$ do not necessarily sum up to the total area change ($\Delta A_{C \to O}$).

RESULTS

To determine the electrophysiological characteristics of MscCG as a mechanosensitive channel as well as a

glutamate exporter, were performed the inside-out, excised patch-clamp method in a symmetric glutamate solution containing 200 mM K-glutamate and a base salt mix (90 mM $MgCl_2$, 10 mM $CaCl_2$, and 5 mM HEPES-KOH, pH 7.2). MscCG was expressed in the *E. coli* strain MJF612, which lacks four endogenous mechanosensitive channels (YbdG, MscS, MscK, and MscL) (7). When a ramp of negative pressure was applied to the patch membrane, mechanosensitive currents of MscCG were triggered at ~100 mmHg and saturated at ~250 mmHg (Fig. 2 *A*). The unit channel currents of MscCG were 6 pA and −3 pA at pipette potentials of +40 mV and −40 mV, respectively. The I/V curve showed that the unitary conductance of MscCG was larger at the positive pipette potential than the negative potential, indicative of voltage-dependent rectification, as reported previously (12). The unitary conductances calculated from the slopes at positive and negative potentials were 155 ± 14 pS and 80 ± 8 pS ($n = 5$), respectively (Fig. 2 *B*).

Because MscCG functions as a glutamate exporter in *C. glutamicum* cells, we examined whether MscCG has a preference for glutamate. In an asymmetric solution containing 200 mM/20 mM K-glutamate (bath/pipette) and the base salt mix, the reversal potential of MscCG shifted slightly to the negative potential, that is, in the direction toward the equilibrium potential for glutamate (−58 mV) rather than potassium (+58 mV) (Fig. 2 *B*). Although the shift was too small to determine the glutamate selectivity of MscCG accurately, P_K/P_{Glu} was estimated to be ~2. The unitary conductances at positive and negative pipette potentials in a symmetric KCl solution (200 mM KCl and the base salt mix), with which most of the experiments on MscS were conducted, were 340 ± 24 pS and 145 ± 9 pS, respectively ($n = 5$; Fig. 2 *C*; Table 1). The increase in conductance with KCl concentration is consistent with a previous study (12). The conductance of MscCG in this symmetric KCl solution is significantly smaller than that of MscS (~1 nS).

The conductance in a symmetric solution of the base salt mix was 153 ± 10 pS and 38 ± 4 pS at positive and negative pipette potentials, respectively ($n = 5$) (Table 1). The conductance at positive pipette potentials was comparable to that in the K-glutamate solution, indicating that neither potassium nor glutamate ions permeate at positive potentials, although the larger conductance at negative potentials in K-glutamate solution indicates permeation of these ions. Considering that the base salt mix contains 200 mM Cl^-, the doubling of conductance at positive potentials by addition of 200 mM KCl to the base salt mix is mostly attributable to the chloride conductance (Table 1). The larger increase in conductance at negative pipette potentials indicates the permeation of potassium ions. Although glutamate poorly permeates the pore from the cytoplasmic side, we conducted the experiments described below at positive pipette potentials because it is difficult to assume that continuous glutamate secretion occurs at negative pipette potentials (i.e., when the membrane potential is depolarized).

To determine the tension needed to activate MscCG, we compared the midpoints of the activation curves of MscCG and MscL in the same patch membrane of PB113 cells, which express endogenous *mscL*. The midpoint tension for the activation of MscL is 11.8 mN/m (8) and was used as an internal standard in this experiment. Note that the activation of mechanosensitive channels depends on membrane tension rather than pressure applied to the membrane, and thus mechanosensitive channels with known tension sensitivity have been coexpressed as an internal standard for calibration in a number of previous studies (27–29). A series of 4-s pulses with increasing pressure were applied to the patch membrane expressing MscCG. Pulses, rather than a ramp, were used to avoid the influence of possible time-dependent adaptation and slow kinetics. Currents generated by MscCG were first elicited at ~50 mmHg (trace 5 in Fig. 3 *A*) and reached saturation at ~80 mmHg (trace 8). Currents generated by MscL started at ~110 mmHg (trace 11). The relationship between the applied pressure and the maximum current depicted activation curves with different midpoints, indicative of a biphasic current response from channel populations of MscCG and MscL (Fig. 3 *B*). The activation curves fitted well with the Boltzmann equation, and the midpoints of activation (P_{mid}), at which a current is half of a saturated current, were 61 mmHg for MscCG and 118 mmHg for MscL. The ratio of P_{mid} of MscCG to that of MscL obtained from four independent experiments was 0.56 ± 0.05. Thus, the activation midpoint of MscCG calculated using the activation midpoint of MscL (11.8 mN/m) is estimated to be 6.7 ± 0.6 mN/m. This result shows that MscCG opens at a tension comparable to that observed for MscS (5–8 mN/m) (5,6,30).

The *E. coli* MscS has been characterized by a quick response to changes in membrane tension and subsequent closure under sustained tension. To compare the gating kinetics between MscCG and MscS, we applied 4-s pulses to MscCG or MscS expressed in *E. coli* MJF612 cells. As reported previously, the current of MscS rose almost simultaneously with pressure application, but declined gradually when the pressure was held at a level around the activation midpoint (trace 7 of MscS in Fig. 4 *A*). In contrast, the current of MscCG rose slowly to a plateau and it took >1 s to reach the plateau at a moderate pressure (trace 4 of MscCG in Fig. 4 *A*). Moreover, the current of MscCG did not decline at any pressure.

The relationship between maximum currents and the applied pressure was plotted and fitted with the Boltzmann distribution function. Assuming that the P_{mid} values of MscCG and MscS are 6.7 mN/m and 5.5 mN/m (30), respectively, we calculated the energy gap between the open and closed states (ΔE) and the in-plane area change (ΔA) of MscCG (see Materials and Methods). ΔE and ΔA were 7.8 ± 2.0 kT and 4.8 ± 1.3 nm^2, respectively, in MscCG

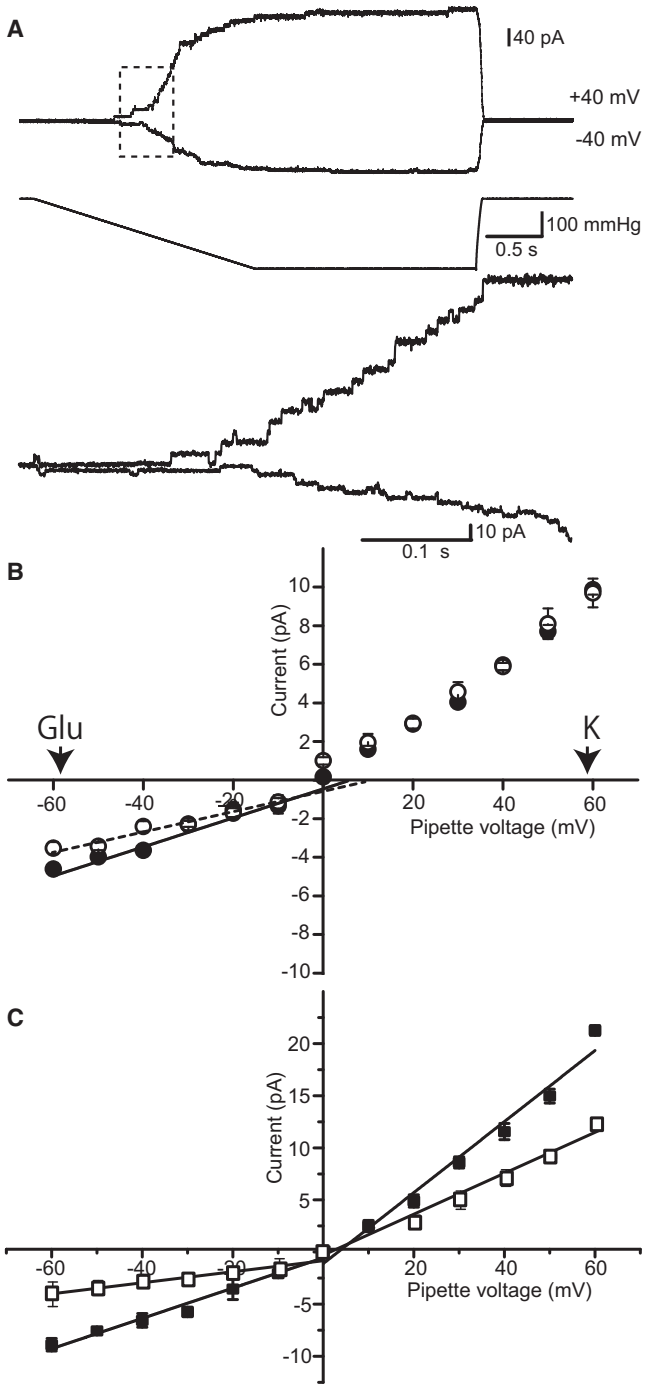

FIGURE 2 Electrophysiological characteristics of MscCG. (*A*) Currents of MscCG expressed in MJF612 strain in a symmetric solution of 200 mM K-glutamate and a base salt mix (90 mM $MgCl_2$, 10 mM $CaCl_2$, 5 mM HEPES-KOH, pH7.2). The pipette potential was held at +40 mV and −40 mV. Traces at the bottom present an expanded view of the dashed box in the traces at the top. (*B*) Current-voltage relationships in symmetric solution (pipette 200 mM/bath 200 mM K-glutamate + base salt mix) (*solid circles*) and asymmetric solution (pipette 20 mM/bath 200 mM K-glutamate + base salt mix) (*open circles*). Conductances of MscCG calculated from the slope of the curve in the symmetric solution were 156 ± 14 pS (positive pipette potential) and 80 ± 8 pS (negative pipette potential; $n = 5$). Reversal potentials are calculated from the intercept of the curve in the negative potential range. Equilibrium potentials for glutamate and potassium by the Nernst equation in the asymmetric solution are shown by arrowheads. (*C*) Current-voltage relationships in symmetric solutions of the base salt mix (*open squares*; $n = 4$) and 200 mM KCl + the base salt mix (*solid square*; $n = 5$). Bars show standard deviation (SD).

($n = 8$), whereas ΔE was 22.4 ± 2.8 k*T* and ΔA was 16.8 ± 2.0 nm^2 in MscS ($n = 12$; Fig. 4 *B*; Table 2). The values for MscS are consistent with previous studies (4,31). This result indicates that MscCG opening is accompanied by a smaller in-plane expansion and requires less energy to gate compared with MscS.

Because the above recordings suggest slow gating kinetics of MscCG, we quantitatively measured the opening and closing rates of MscCG. Pressure was controlled using P_{mid} as a reference so that data from different patch membranes could be assembled for statistical analysis. Fig. 5 *A* shows the response of MscCG and MscS to various pressure levels followed by a supramaximal pulse ($2\times P_{mid}$). The pressure at the beginning was increased by $0.2\times P_{mid}$. Obviously, MscCG opened gradually, whereas MscS opened almost instantaneously. The red lines represent single-exponential functions fitted to the traces, and the opening time constant (τ) is shown in Fig. 5 *C*. The opening time constant of MscCG was on the order of hundreds of milliseconds. An exponential fit to the opening of MscS has a time constant of ~10 ms, but this is likely to be defined by the rate of increase in pressure, which took up to 10 ms to reach the maximum. Thus, the rate close to 10 ms was excluded from further analysis. Nevertheless, given that the time constant of the opening of MscS is <10 ms, one can conclude that the rate of opening of MscCG is slower than that of MscS by one order of magnitude or more. We analyzed the closing kinetics of MscCG and MscS by applying a supramaximal pulse ($2\times P_{mid}$), which opened the entire channel population (>500 channels) in the patch membranes, and reducing the pressure to various levels (Fig. 5 *B*). Again, the change in currents was much faster in MscS than in MscCG. The closing time constants of MscCG was consistently larger than MscS at stimulus levels from $0.6 \times P_{mid}$ to $1.0 \times P_{mid}$, suggesting that MscCG has slower closing kinetics than MscS (Fig. 5 *C*). A large number of channels are likely due to the strong promoter used for induction. Note also that the number of MscL channels per cell expressed under native promoter depends strongly on the culturing conditions and stress factors (32).

The inverse of the time constant (τ) for opening and closing represents the rate constant for opening (k_{on}) and closing (k_{off}). Using the correlation between these rate constants and tension, we calculated the changes in the in-plane area from the closed (C) to the energy barrier nearest to the closest state (BC) ($\Delta A_{C\rightarrow BC}$) and that from the open (O) state to the energy barrier nearest to the open state (BO) ($\Delta A_{O\rightarrow BO}$). $\Delta A_{C\rightarrow BC}$ was 0.5 nm^2 and $\Delta A_{O\rightarrow BO}$ was 2.4 nm^2 in MscCG. $\Delta A_{O\rightarrow BO}$ was 3.8 nm^2 in MscS, which is largely consistent with a previous report (9).

TABLE 1 Bulk conductivity of solution and conductance of MscCG in the symmetric solutions

Solution	Bulk conductivity	Conductance	
		Positive potential[a]	Negative potential[a]
Base salt mix[b]	19.4 mS/cm	153 ± 10 pS	38 ± 4 pS
Mix+200 K-Glu[c]	31.3 mS/cm	155 ± 14 pS	80 ± 8 pS
Mix+200 KCl[d]	40.1 mS/cm	340 ± 24 pS	145 ± 9 pS

[a]Pipette potential.
[b]90 mM $MgCl_2$, 10 mM $CaCl_2$, 5 mM HEPES-KOH pH 7.2.
[c]200 mM K-glutamate + base salt mix.
[d]200 mM KCl + base salt mix.

Because hysteresis gating has been reported in the *Arabidopsis* and *Chlamydomonas* MscS homologs MSL10 and MSC1 as a characteristic of eukaryotic MscS homologs (33,34), we analyzed whether MscCG shows hysteresis gating. If the gating kinetics is too slow to follow changes in stimulus intensity, or the gating mechanisms of opening and closing differ, mechanosensitive channels may show hysteretic behavior in response to ascending and descending stimuli, and different thresholds for opening and closing. We compared the hysteretic characteristics of MscCG and MscS by applying ascending and descending pressures at various ramp rates. The currents of MscCG and MscS expressed in *E. coli* MJF612 cells were recorded under a trapezoidal pressure protocol at ramp rates of 2 × P_{mid} mmHg/1 s to 2 × P_{mid} mmHg/8 s, and the activation curves of opening and closing were fitted by the Boltzmann equation (Fig. 6 *A*). At a high ramp rate (2 × P_{mid} mmHg/1 s), MscCG opened and closed during the latter half of the ramp; the midpoint of opening (~230 mmHg) was significantly higher than that of closing (~100 mmHg; Fig. 6 *A*, *top*). MscS also showed some hysteretic characteristics, but to a much smaller extent than MscCG. The midpoints for opening and closing approached each other when the ramp rate was decreased, and the curves for opening and closing almost coincided at the lowest ramp rate examined (2 × P_{mid} mmHg/8 s; Fig. 6 *A*, *bottom*). The midpoints for opening and closing were normalized by P_{mid} as determined

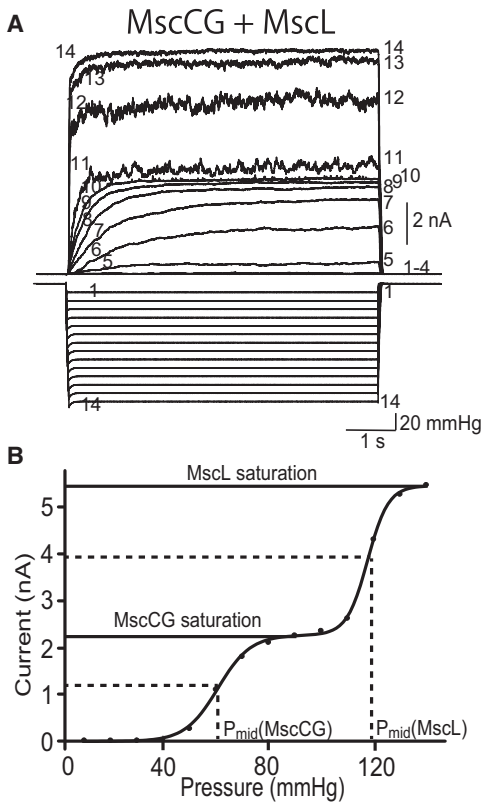

FIGURE 3 Threshold of membrane tension in MscCG. (*A*) Currents of MscCG in the PB113 strain (Δ*mscS* and Δ*mscK*). Four-second pressure pulses with various amplitudes were applied to the patch membrane at a pipette potential of +40 mV. Current generated by MscCG was elicited at a low pressure, and current generated by MscL was activated at a higher pressure. The numbers in the current and pressure traces correspond to each other. (*B*) Relationship between pressure and the maximum current. P_{mid} of MscCG and MscL was determined by fitting to Boltzmann functions. The ratio of P_{mid} of MscCG to P_{mid} of MscL was 0.56 ± 0.05 (n = 4).

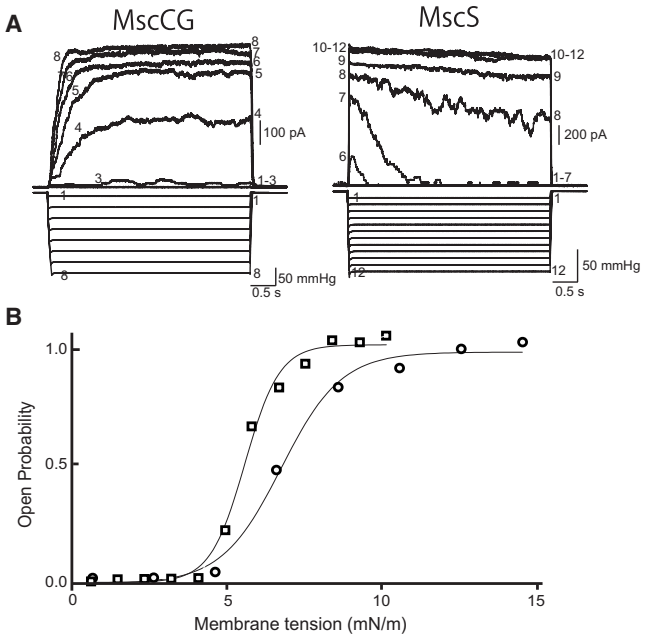

FIGURE 4 Activation curves of MscCG and MscS. (*A*) Currents generated by MscCG and MscS in the MJF612 strain when 4-s pressure pulses were applied to the patch membrane in 200 mM K-glutamate and the base salt mix at a pipette potential of +40 mV. The numbers in the current and pressure traces correspond to each other. (*B*) Activation curve of MscCG (*circles*) and MscS (*squares*). P_{mid} of MscCG and MscS was determined by fitting to Boltzmann functions. The energy gap between the open and closed states (ΔE) and the in-plane area change (ΔA) obtained from the Boltzmann functions are listed in Table 2.

TABLE 2 Energetic and spatial parameters of MscCG and MscS

	P_{mid} (mmHg)	$1/\alpha$ (mmHg^{-1})	ΔE (kT)	ΔA (nm^2)
MscCG (n = 8)	107 ± 35	13.8 ± 4.2	7.8 ± 2.0	4.8 ± 1.3
MscS (n = 12)	94 ± 12	4.2 ± 0.5	22.4 ± 2.8	16.8 ± 2.0

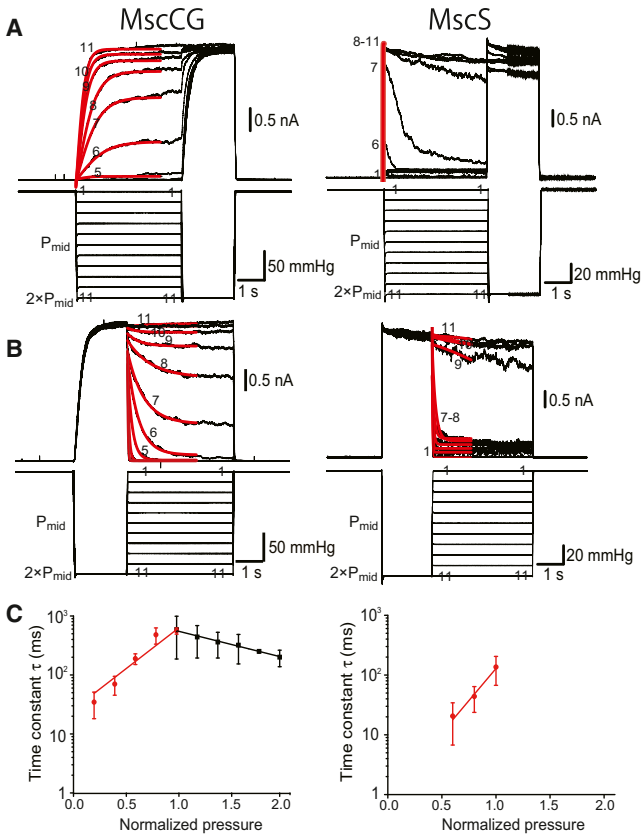

FIGURE 5 Opening and closing rates of MscCG and MscS. (*A*) Rate of opening at various pressures. Pressure with various magnitudes was applied first and was followed by a supramaximal pulse. Pressure was changed in steps of 0.2 × P_{mid}, where P_{mid} is the midpoint of the activation curve. Red lines show single-exponential fitting. (*B*) Rate of closing at various pressures. A supramaximal pulse was applied first to activate all channels, followed by pressure with various magnitudes. (*C*) Time constants (τ) for opening (*black*) and closing (*red*) in MscCG (*left*) and MscS (*right*) were plotted ($n = 3$). All data were taken in the MJF612 strain in 200 mM K-glutamate and the base salt mix at a pipette potential of +40 mV. Bars show SD.

by a pulse protocol and were plotted against the ramp rate (Fig. 6 *B*). At the ramp rate of 2 × P_{mid} mmHg/1 s, normalized midpoints for the opening and closing of MscCG were 1.66 ± 0.21 and 0.69 ± 0.12 ($n = 3$), whereas those of MscS were 1.16 ± 0.03 and 0.91 ± 0.08 ($n = 3$), respectively. The dissociation of the midpoints of opening and closing largely disappeared when the ramp rate was reduced to 2 × P_{mid} mmHg/8 s. The midpoint of opening was also greater than that of closing in MscS, but the difference was smaller than that of MscCG. These findings suggest that MscCG has stronger hysteretic characteristics than MscS.

Currents due to MscS are known to decay at sustained pressure in excised patches, and the decay has been attributed to inactivation (channels do not open even at supramaximal pressure) and desensitization (channels reopen when supramaximal pressure is applied). Desensitization occurs only in the excised patch and is absent in the whole-cell configuration, suggesting that desensitization is due to relaxation of tension in one of the membrane monolayers (5). These processes occur in a tension-dependent manner (35). We examined whether MscCG also has such adaptive mechanisms. After the first saturating pulse at 2 × P_{mid}, we kept the pressure at various levels for 30 s to examine the pressure dependence of the current decay. The second saturating pulse at 2 × P_{mid} was applied at the end to test whether the channels were inactivated. Regardless of the pressure between the two pulses, full activation was induced by the second pulse in MscCG, indicating that MscCG was not inactivated at any pressure (Fig. 7 *A*). In contrast, the response to the second pulse was greatly reduced in MscS at the intervening pressure of 1 × P_{mid} or higher (traces 6 and 7 of MscS in Fig. 7 *A*). The inactivation rates of MscCG and MscS were evaluated by the ratio of currents evoked by the second pulse to those by the first pulse (Fig. 7 *B*). The inactivation rate of MscCG was ~1 at any intervening pressure, confirming full activation by the second pulse. However, more than half of the MscS was inactivated at an intervening pressure of 1 × P_{mid} or higher, indicative of pressure-dependent inactivation. These observations suggest that MscCG does not have a mechanism of inactivation, which is an important characteristic of MscS as an osmotic safety valve (9).

A crystal structure (36) of MscS has a kink at Gly-113 located in the pore-forming helix TM3 (Fig. 1, *A* and *C*). Substitution of this residue with an amino acid with a large side chain, which should reduce the flexibility of the TM3 helix at this residue, results in a remarkable loss of inactivation (37). For example, the G113A mutant does not undergo inactivation, and the viability of cells with the mutation is decreased significantly upon a long hypoosmotic shock (9,37). MscCG has serine at this position (Fig. 1 *C*), suggesting that loss of inactivation may be due to a decrease in flexibility at this position. To test whether an absence of glycine at this position prevents the gating transition to inactivation, we introduced two glycine residues at this and adjacent residues. However, this mutant, Q112G S113G, was not inactivated as with the wild-type MscCG, indicating that the lack of inactivation should be attributable to another region (Fig. 7 *C*).

DISCUSSION

MscCG has a dual function of glutamate secretion and osmoregulation in *C. glutamicum* cells. In this study, we characterized electrophysiologically the mechanosensitive gating kinetics of MscCG expressed in *E. coli* giant spheroplasts. MscCG was a mechanosensitive channel with an activation midpoint of 6.7 ± 0.6 mN/m and was permeable to glutamate. MscCG had remarkably slower gating kinetics than MscS and displayed strong hysteretic gating properties. MscCG did not have a mechanism of inactivation, whereas

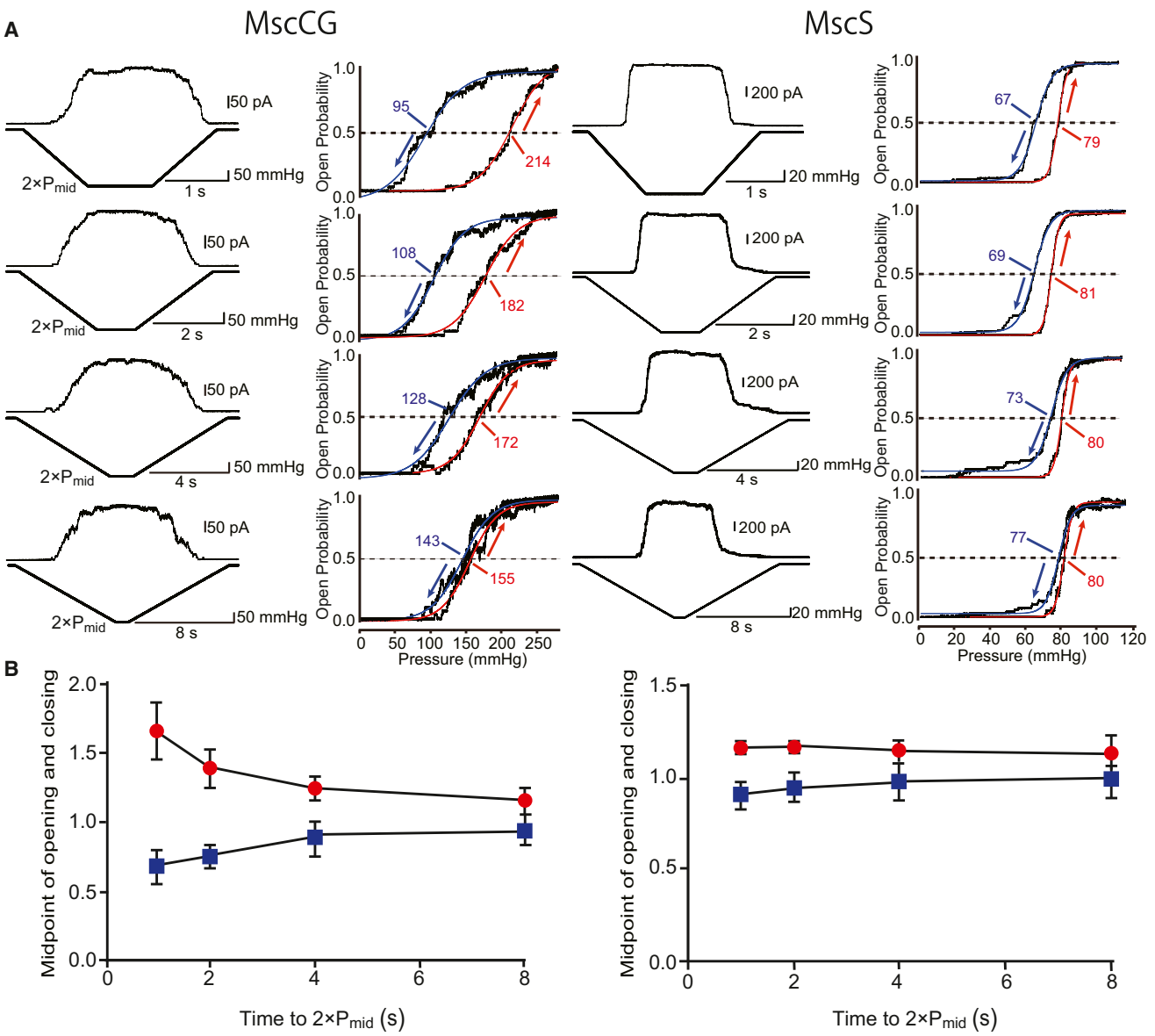

FIGURE 6 Hysteretic gating behaviors of MscCG and MscS. (*A*) Current and pressure (*left*) in the response to pressure ramps at 2 × P_{mid}/1 s to 2 × P_{mid}/8 s. Pressure was changed from 0 to 2 × P_{mid} or vice versa over 1- to 8-s ramps. The pressure versus open probability relationships in opening (*red*) and closing (*blue*) transitions were fitted with the Boltzmann functions, and the activation midpoint (P_{mid}) was determined (*right*). Red and blue arrows show the kinetics of opening and closing, respectively. (*B*) Ramp-rate dependence of gating midpoints. P_{mid} values determined in ramp experiments were normalized by P_{mid} values determined in pulse experiments and were plotted against the ramp rate. The midpoints for opening (*red*) and closing (*blue*) are shown ($n = 3$). All data were taken in the MJF612 strain in 200 mM K-glutamate and the base salt mix at a pipette potential of +40 mV. Data were acquired at ≤90-s intervals to ensure recovery from the inactivated state to the resting state. Bars show SD.

MscS's adaptation enabled it to avoid constant flickering under sustained stimuli.

Fast gating kinetics enables MscS to respond to sudden osmotic challenges. Whereas osmotic pressure rises in *E. coli* cells within 30–50 ms after an abrupt hypoosmotic shock, MscS opens within 20 ms, as shown by stopped-flow and patch-clamp analyses (9). In contrast, the opening time constant of MscCG determined in this study was on the order of hundreds of milliseconds, which is at least 10 times slower than that of MscS. Thus, MscCG probably cannot open before osmotic pressure builds up to a lytic level when an abrupt osmotic downshock is applied. Considering this slow kinetics, MscCG would be a poor safety valve. *C. glutamicum* has a single MscL homolog (NCgl0843), but cells devoid of this MscL homolog and MscCG still survive hypoosmotic shock (38), indicating that osmotic regulators other than MscCG and MscL homolog may exist.

In *E. coli* cells, inactivation of MscS is required for survival upon hypoosmotic shock to prevent excessive efflux of small molecules and to facilitate recovery (9). The lack

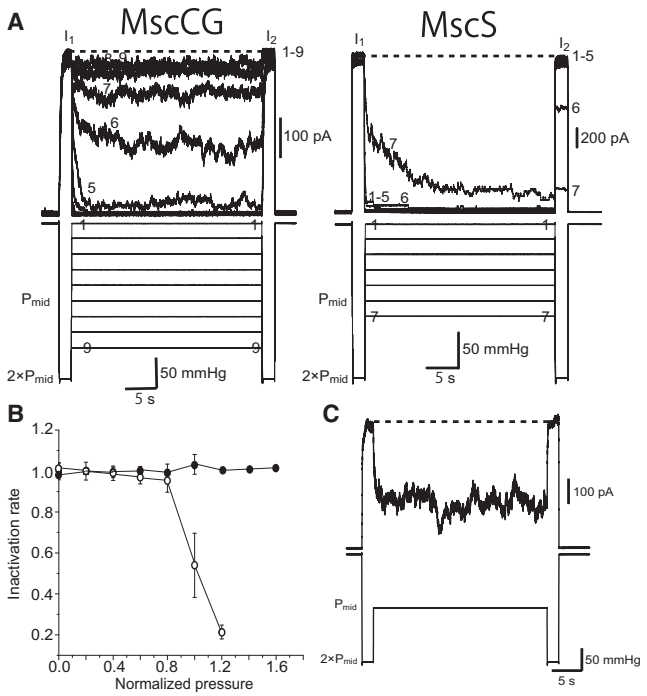

FIGURE 7 Inactivation of MscCG and MscS. (*A*) Responses to two 2-s supramaximal pulses ($2 \times P_{mid}$) separated by 30-s pressure. The intervening pressure was increased by $0.2 \times P_{mid}$. The numbers in the current and pressure traces correspond to each other. (*B*) The ratio of the currents generated by the first and second pulses is plotted as the inactivation rate of MscCG (*solid circles*) and MscS (*open circles*; $n = 5$). (*C*) Current response of Q112G S113G mutant of MscCG to the paired-pulse protocol. All data were taken in the MJF612 strain in 200 mM K-glutamate and the base salt mix at a pipette potential of +40 mV. Bars show SD.

of inactivation in MscCG implies that cytoplasmic solutes will be lost as long as the hypoosmotic shock persists. Thus, it is possible that, in contrast to the opening of MscS, opening of MscCG could be fatal upon hypoosmotic shock. However, the fact that *C. glutamicum* cells lacking MscCG do not die upon hypoosmotic shock implies that MscCG would not be a safety valve. A recent study revealed that MscSP, an MscS homolog of the sulfur-compound-decomposing, Gram-negative marine bacterium *Silicibacter pomeroyi*, also does not inactivate when it is expressed in *E. coli* cells and reconstituted in liposomes (39). MscSP may have a physiological role unrelated to osmotic response, as is the case with MscCG. Note, however, that the absence of inactivation in a heterogeneous expression system does not totally exclude the occurrence of inactivation in vivo.

Introduction of glycine residues at the kink-forming position in MscS did not give rise to inactivation, indicating that the lack of inactivation is not due to the absence of glycine, or flexibility, at this position. Besides the kink at TM3, an electrostatic interaction between the carboxyl end of TM3 (Arg-128 and Arg-131) and Asp-62 in the loop between TM1 and TM2 (Fig. 1 *C*) is also known to affect inactivation critically (40). Loss of this electrostatic interaction results in an increased rate of inactivation, indicating that a salt bridge is present in the open state but is dissociated in the inactivated state. Loss of this connection also reduces swelling of the cytoplasmic cage, which occurs upon opening (41). Curiously, this electrostatic interaction is probably absent in MscCG because Asp-62 and Arg-131 in MscS are replaced by phenylalanine and glycine residues, respectively. The absence of inactivation, despite the absence of the electrostatic interaction between the TM domain and the cytoplasmic cage, suggests that coordinated motion of the TM domain and the cytoplasmic cage of MscCG is achieved through a mechanism different from that of MscS.

C. glutamicum responds to hypoosmotic shock by an efflux of compatible solutes, in particular glycine betaine (42). Consequently, the export of amino acids such as glutamate and lysine is restricted. On the other hand, incubation of *C. glutamicum* cells under biotin limitation results in excretion of a large amount of glutamate. Biotin limitation causes reduced fatty acid synthesis, resulting in reduction of the amount of mycolic acid and continuous alteration of membrane tension (19). Given that MscCG is not selective for glutamate, constitutive opening of MscCG should cause excessive efflux of cytoplasmic solutes during glutamate production. *C. glutamicum* may have an auxiliary regulatory system for the prevention of excessive efflux of cytoplasmic solutes. However, further studies are needed to elucidate this possibility.

The conductances of MscCG at positive and negative potentials were 155 and 80 pS, respectively, which are significantly smaller than those of MscS (~1 nS; Table 1). Consistent with the reduced conductance, the in-plane area change upon gating (ΔA) was reduced from 16.8 nm^2 (MscS) to 4.8 nm^2 (MscCG), indicative of a smaller conformational change in MscCG. The in-plane area changes from the closed state to the nearest barrier ($\Delta A_{C \rightarrow BC}$) were almost comparable (2.1 nm^2 for MscCG and 2.9 nm^2 for MscS). The change from the open state to the nearest barrier ($\Delta A_{O \rightarrow BO}$) observed in this study (0.5 nm^2 for MscCG) was also close to the value reported previously for MscS (0.5 nm^2) (9). The similarities of these transition parameters suggest that critical steps for gating transition are conserved between MscS and MscCG.

The similarity of $\Delta A_{O \rightarrow BO}$ between MscCG and MscS reflects the similarity of the slope of the closing rate (or time constant) when plotted against pressure (or tension; Fig. 5 *C*). Thus, the slow closing rate of MscCG is likely due to a parallel shift of the closing rate curve rather than a change in tension dependence (slope). The intercept of the regression line at pressure = 0 indicates that the closing rates at pressure = 0 are 0.037 ms^{-1} in MscCG and 1.09 ms^{-1} in MscS, suggesting a 30-fold increase in the intrinsic closing rate. Thus, one of the characteristics of MscCG is an intrinsically slow rate of conformational change.

The slow rate of opening and closing should make it difficult for channels to follow rapid changes in stimulus intensity, which is a likely reason for hysteresis. Marked hysteresis has also been reported in eukaryotic MscS homologs of *Arabidopsis thaliana* (MSL10) (33) and *Chlamydomonas reinhardtii* (MSC1) (34). Although the functions of MSC1 and MSL10 are not fully understood, it is unlikely that they are activated directly by osmotic downshock, because MSC1 is localized in the intracellular membranes and MSL10 is expressed in the root cells. Thus, hysteresis and leisurely kinetics may be advantageous for executing slow processes such as metabolism and glutamate secretion by MscCG.

To summarize, slow kinetics and the absence of inactivation in MscCG are not suitable for a response to rapid osmotic downshock. The absence of inactivation in MscCG should be essential for sustained activities such as glutamate excretion. We suggest that MscCG has the properties of a sustainable metabolic valve rather than an osmotic safety valve.

We thank Ajinomoto Co., Inc., for providing information, Dr. Ian Booth and Dr. Akiko Rasmussen for the gift of *E. coli* strain MJF612, and Ms. Yumiko Higashi for secretarial assistance.

This work was supported by Grants-in-Aid for Scientific Research on Priority Areas from the Ministry of Education, Culture, Sports, Science and Technology of Japan (21026009, 23120509 and 25120708 to H.I.); a Grant-in-Aid for Scientific Research B from the Japan Society for the Promotion of Science (JSPS; 21370017 to H.I.); and a Grant-in-Aid for JSPS Fellows (10J02008 to Y.N.).

REFERENCES

1. Li, Y., P. C. Moe, …, P. Blount. 2002. Ionic regulation of MscK, a mechanosensitive channel from *Escherichia coli*. *EMBO J.* 21:5323–5330.
2. Berrier, C., M. Besnard, …, A. Ghazi. 1996. Multiple mechanosensitive ion channels from *Escherichia coli*, activated at different thresholds of applied pressure. *J. Membr. Biol.* 151:175–187.
3. Edwards, M. D., S. Black, …, I. R. Booth. 2012. Characterization of three novel mechanosensitive channel activities in *Escherichia coli*. *Channels (Austin).* 6:272–281.
4. Levina, N., S. Tötemeyer, …, I. R. Booth. 1999. Protection of *Escherichia coli* cells against extreme turgor by activation of MscS and MscL mechanosensitive channels: identification of genes required for MscS activity. *EMBO J.* 18:1730–1737.
5. Belyy, V., K. Kamaraju, …, S. Sukharev. 2010. Adaptive behavior of bacterial mechanosensitive channels is coupled to membrane mechanics. *J. Gen. Physiol.* 135:641–652.
6. Sukharev, S. 2002. Purification of the small mechanosensitive channel of *Escherichia coli* (MscS): the subunit structure, conduction, and gating characteristics in liposomes. *Biophys. J.* 83:290–298.
7. Schumann, U., M. D. Edwards, …, I. R. Booth. 2010. YbdG in *Escherichia coli* is a threshold-setting mechanosensitive channel with MscM activity. *Proc. Natl. Acad. Sci. USA.* 107:12664–12669.
8. Sukharev, S. I., W. J. Sigurdson, …, F. Sachs. 1999. Energetic and spatial parameters for gating of the bacterial large conductance mechanosensitive channel, MscL. *J. Gen. Physiol.* 113:525–540.
9. Boer, M., A. Anishkin, and S. Sukharev. 2011. Adaptive MscS gating in the osmotic permeability response in *E. coli*: the question of time. *Biochemistry.* 50:4087–4096.
10. Malcolm, H. R., and J. A. Maurer. 2012. The mechanosensitive channel of small conductance (MscS) superfamily: not just mechanosensitive channels anymore. *ChemBioChem.* 13:2037–2043.
11. Balleza, D., and F. Gómez-Lagunas. 2009. Conserved motifs in mechanosensitive channels MscL and MscS. *Eur. Biophys. J.* 38:1013–1027.
12. Börngen, K., A. R. Battle, …, R. Krämer. 2010. The properties and contribution of the *Corynebacterium glutamicum* MscS variant to fine-tuning of osmotic adaptation. *Biochim. Biophys. Acta.* 1798:2141–2149.
13. Nakamura, J., S. Hirano, …, M. Wachi. 2007. Mutations of the *Corynebacterium glutamicum* NCgl1221 gene, encoding a mechanosensitive channel homolog, induce L-glutamic acid production. *Appl. Environ. Microbiol.* 73:4491–4498.
14. Becker, M., K. Börngen, …, R. Krämer. 2013. Glutamate efflux mediated by *Corynebacterium glutamicum* MscCG, *Escherichia coli* MscS, and their derivatives. *Biochim. Biophys. Acta.* 1828:1230–1240.
15. Viarouge, C., R. Caulliez, and S. Nicolaidis. 1992. Umami taste of monosodium glutamate enhances the thermic effect of food and affects the respiratory quotient in the rat. *Physiol. Behav.* 52:879–884.
16. Hermann, T. 2003. Industrial production of amino acids by coryneform bacteria. *J. Biotechnol.* 104:155–172.
17. Shiratsuchi, M., H. Kuronuma, …, S. Nakamori. 1995. Simultaneous and high fermentative production of L–Lysine and L-glutamic acid using a strain of *Brevibacterium lactofermentum*. *Biosci. Biotechnol. Biochem.* 59:83–86.
18. Shiio, I., S. I. Otsuka, and M. Takahashi. 1962. Effect of biotin on the bacterial formation of glutamic acid. I. Glutamate formation and cellular premeability of amino acids. *J. Biochem.* 51:56–62.
19. Kim, J., T. Hirasawa, …, H. Shimizu. 2011. Investigation of phosphorylation status of OdhI protein during penicillin- and Tween 40-triggered glutamate overproduction by *Corynebacterium glutamicum*. *Appl. Microbiol. Biotechnol.* 91:143–151.
20. Hashimoto, K., H. Kawasaki, …, T. Nakamatsu. 2006. Changes in composition and content of mycolic acids in glutamate-overproducing *Corynebacterium glutamicum*. *Biosci. Biotechnol. Biochem.* 70:22–30.
21. Hashimoto, K., K. Nakamura, …, H. Kawasaki. 2010. The protein encoded by NCgl1221 in *Corynebacterium glutamicum* functions as a mechanosensitive channel. *Biosci. Biotechnol. Biochem.* 74:2546–2549.
22. Hashimoto, K., J. Murata, …, H. Kawasaki. 2012. Glutamate is excreted across the cytoplasmic membrane through the NCgl1221 channel of *Corynebacterium glutamicum* by passive diffusion. *Biosci. Biotechnol. Biochem.* 76:1422–1424.
23. Nakayama, Y., K. Yoshimura, and H. Iida. 2012. A gain-of-function mutation in gating of *Corynebacterium glutamicum* NCgl1221 causes constitutive glutamate secretion. *Appl. Environ. Microbiol.* 78:5432–5434.
24. Martinac, B., M. Buechner, …, C. Kung. 1987. Pressure-sensitive ion channel in *Escherichia coli*. *Proc. Natl. Acad. Sci. USA.* 84:2297–2301.
25. Besch, S. R., T. Suchyna, and F. Sachs. 2002. High-speed pressure clamp. *Pflugers Arch.* 445:161–166.
26. Anishkin, A., C. S. Chiang, and S. Sukharev. 2005. Gain-of-function mutations reveal expanded intermediate states and a sequential action of two gates in MscL. *J. Gen. Physiol.* 125:155–170.
27. Edwards, M. D., Y. Li, …, I. R. Booth. 2005. Pivotal role of the glycine-rich TM3 helix in gating the MscS mechanosensitive channel. *Nat. Struct. Mol. Biol.* 12:113–119.
28. Nomura, T., M. Sokabe, and K. Yoshimura. 2006. Lipid-protein interaction of the MscS mechanosensitive channel examined by scanning mutagenesis. *Biophys. J.* 91:2874–2881.
29. Nomura, T., C. G. Cranfield, …, B. Martinac. 2012. Differential effects of lipids and lyso-lipids on the mechanosensitivity of the mechanosensitive channels MscL and MscS. *Proc. Natl. Acad. Sci. USA.* 109:8770–8775.

30. Kamaraju, K., P. A. Gottlieb, …, S. Sukharev. 2010. Effects of GsMTx4 on bacterial mechanosensitive channels in inside-out patches from giant spheroplasts. *Biophys. J.* 99:2870–2878.

31. Akitake, B., A. Anishkin, and S. Sukharev. 2005. The "dashpot" mechanism of stretch-dependent gating in MscS. *J. Gen. Physiol.* 125:143–154.

32. Bialecka-Fornal, M., H. J. Lee, …, R. Phillips. 2012. Single-cell census of mechanosensitive channels in living bacteria. *PLoS ONE.* 7:e33077.

33. Maksaev, G., and E. S. Haswell. 2012. MscS-Like10 is a stretch-activated ion channel from *Arabidopsis thaliana* with a preference for anions. *Proc. Natl. Acad. Sci. USA.* 109:19015–19020.

34. Nakayama, Y., K. Fujiu, …, K. Yoshimura. 2007. Molecular and electrophysiological characterization of a mechanosensitive channel expressed in the chloroplasts of *Chlamydomonas*. *Proc. Natl. Acad. Sci. USA.* 104:5883–5888.

35. Kamaraju, K., V. Belyy, …, S. Sukharev. 2011. The pathway and spatial scale for MscS inactivation. *J. Gen. Physiol.* 138:49–57.

36. Bass, R. B., P. Strop, …, D. C. Rees. 2002. Crystal structure of *Escherichia coli* MscS, a voltage-modulated and mechanosensitive channel. *Science.* 298:1582–1587.

37. Akitake, B., A. Anishkin, …, S. Sukharev. 2007. Straightening and sequential buckling of the pore-lining helices define the gating cycle of MscS. *Nat. Struct. Mol. Biol.* 14:1141–1149.

38. Nottebrock, D., U. Meyer, …, S. Morbach. 2003. Molecular and biochemical characterization of mechanosensitive channels in *Corynebacterium glutamicum*. *FEMS Microbiol. Lett.* 218:305–309.

39. Petrov, E., D. Palanivelu, …, B. Martinac. 2013. Patch-clamp characterization of the MscS-like mechanosensitive channel from *Silicibacter pomeroyi*. *Biophys. J.* 104:1426–1434.

40. Nomura, T., M. Sokabe, and K. Yoshimura. 2008. Interaction between the cytoplasmic and transmembrane domains of the mechanosensitive channel MscS. *Biophys. J.* 94:1638–1645.

41. Machiyama, H., H. Tatsumi, and M. Sokabe. 2009. Structural changes in the cytoplasmic domain of the mechanosensitive channel MscS during opening. *Biophys. J.* 97:1048–1057.

42. Ruffert, S., C. Lambert, …, R. Krämer. 1997. Efflux of compatible solutes in *Corynebacterium glutamicum* mediated by osmoregulated channel activity. *Eur. J. Biochem.* 247:572–580.